Mapping the Oceanic Mesoscale Circulation: Validation of Satellite Altimetry Using Surface Drifters

P. Y. LE TRAON AND F. HERNANDEZ

CLS Argos, Toulouse, France

3 August 1991 and 11 March 1992

ABSTRACT

This study aims to show that Lagrangian surface drifters are a suitable means of validating the mapping of oceanic mesoscale circulation by satellite altimetry. Tests are done using Geosat data to simulate drifter trajectories in the Azores–Madeira area. Multivariate objective analysis is then done to estimate the dynamic topography and its associated formal error using the velocity measurements obtained along drifter trajectories. This dynamic-topography field is compared with the reference field as given by Geosat data. Sensitivity to drifter number and energy level is studied. It is shown that with 25 drifters in a 500-km × 500-km area, the dynamic topography is obtained to within a formal accuracy of around 10%–20%. The difference between the estimated and reference fields is below 2 cm rms. These errors are smaller than the mapping errors induced by the space–time sampling of *ERS-1* or TOPEX-POSEIDON satellites. According to these preliminary results, surface drifters are an efficient tool for validating mesoscale mapping by altimetry. More generally, the study shows that by comparing satellite altimetry with data from sufficient surface drifters, the differences between the signals can be estimated.

1. Introduction

By providing global coverage in space and time, satellite altimetry is a unique tool for mapping the oceanic mesoscale circulation. This capability has been extensively used in the past to study eddy dynamics almost everywhere in the world (e.g., De Mey and Menard 1989; Gordon and Haxby 1990; White et al. 1990). The mapping of oceanic mesoscale circulation by altimetry is, however, error prone for several reasons. First, altimetric measurements are noisy and the necessary environmental corrections are not perfectly known (e.g., Tapley et al. 1982; Cheney et al. 1987). Conventional methods of correcting orbit error can also induce discrepancies between adjacent tracks and directly impact the mapping (Le Traon et al. 1991). In addition, along-track sampling implies synoptic mapping by space–time interpolation, which is another major source of error. In situ measurements are therefore needed for validation. This is one of the goals of the Semaphore experiment (Eymard 1991) to be conducted in the Azores–Madeira area in mid-1993. It is thought that Lagrangian surface drifters drogued below the mixed layer are a suitable means of providing such validation (e.g., Willebrand et al. 1990). These drifters, if properly designed to reduce the wind and wave effects (e.g., Niiler et al. 1987; Booth 1989), can indeed be precise geostrophic current followers (to within less than 2 cm s^{-1}).

The purpose of this study is to quantify the contribution drifters can make to describing mesoscale features, and to estimate the number needed to validate satellite altimetry. Geosat altimeter data have been processed and used to simulate drifting-buoy trajectories in the Azores–Madeira region in an area of 500 km × 500 km centered on 33°N, 23°W. The dynamic surface topography and its formal error are then calculated by objective analysis of the along-trajectory velocity measurements. To quantify the drifters' contribution, the data are compared with the Geosat altimeter reference topography and formal mapping errors are analyzed. Section 2 describes the methods and results are presented in section 3. Formal errors are also compared with those expected from the *ERS-1* and/or TOPEX-POSEIDON satellites in section 4. Section 5 provides the main conclusions.

2. Methods

a. Mapping dynamic topography from Geosat data

We simulated the surface-drifter trajectories from Geosat altimeter data (Cheney et al. 1987). These data provide fairly accurate mapping of the variable part of the surface mesoscale dynamic topography. Two-and-a-half years of Geosat altimeter data were processed (November 1986–February 1989), that is, 57 17.05-day cycles. The variable part of the dynamic topogra-

Corresponding author address: Dr. P. Y. Le Traon, CLS Argos, 18 Avenue Edouard Belin, 31055 Toulouse, France.

phy (referred to hereafter as H) was obtained by the conventional repeat-track method, described in detail in a number of papers, for example, Le Traon et al. (1990).

The two-dimensional fields were mapped by objective analysis (e.g., De Mey and Menard 1989) from the ϕ_{obs^i} observations of the along-track dynamic topography H. The optimal estimation $H_{\text{est}}(\mathbf{x})$ ($\mathbf{x} = x_1, x_2$) and its quadratic error $e^2(\mathbf{x})$ are given by Bretherton et al. (1976). First, let us restate the conventional formulas:

$$H_{\text{est}}(\mathbf{x}) = \sum_{i=1}^{N} \sum_{j=1}^{N} A_{ij}^{-1} C_{\mathbf{x}j} \phi_{\text{obs}^i} \quad (1)$$

$$e^2(\mathbf{x}) = C_{\mathbf{xx}} + \sum_{i=1}^{N} \sum_{j=1}^{N} C_{\mathbf{x}i} C_{\mathbf{x}j} A_{ij}^{-1} \quad (2)$$

$\phi_{\text{obs}^i} = \phi_i + \epsilon_i$ (ϕ_{obs^i} is the true value ϕ_i plus noise ϵ_i). Matrices **A** and **C** are the covariance matrices of, respectively, the observations with respect to each other and the observations with respect to the field to be estimated. Thus,

$$A_{ij} = \langle \phi_{\text{obs}^i} \phi_{\text{obs}^j} \rangle = \langle \phi_i \phi_j \rangle + \langle \epsilon_i \epsilon_j \rangle$$

$$C_{\mathbf{x}i} = \langle H(\mathbf{x}) \phi_{\text{obs}^i} \rangle = \langle H(\mathbf{x}) \phi_i \rangle$$

$\langle \epsilon_i \epsilon_j \rangle$ is the noise covariance matrix, assumed here to be diagonal (i.e., the ϵ_i values are not correlated with each other). The ϵ_i values are also assumed to be noncorrelated with the H field to be estimated, that is, $\langle \epsilon_i H(\mathbf{x}) \rangle = 0$. In practice, such an analysis is suboptimal and uses only measurements sufficiently well correlated with the estimation point. We did space–time analysis. The space–time covariance function is the isotropic space covariance function put forward by Arhan and Colin de Verdière (1985), multiplied by a Gaussian temporal decreasing function, as follows:

$$C(r, t) = \text{var}H\left[1 + ar + \frac{1}{6}(ar)^2 - \frac{1}{6}(ar)^3\right] \times \exp(-ar) \exp\left(\frac{-t^2}{T^2}\right); \quad (3)$$

$r = (x_1^2 + x_2^2)^{1/2}$ is the spatial lag, t the temporal lag, and var$H$ the variance of dynamic topography, which does not need to be known for objective analysis.

The noise level (noise variance divided by signal variance) was set a priori at 15%, which corresponds to 2–3 cm rms noise for an H variance of 40 cm^2 typical of the low-energy areas of the ocean. Note that prior to the objective analysis, a low-pass filter is applied to Geosat data (Lanczos filter with a cutoff wavelength of 100 km) so that the instrumental noise is considerably reduced. Parameter a was set at 40 km^{-1}, for a first zero crossing by C of 135 km. This scale is typical of mesoscale eddies at midlatitudes, as obtained from Geosat data (Le Traon et al. 1990). Parameter T was set at 25 days, also estimated from Geosat data (Le Traon 1991).

Mappings were done every 20 days, starting on 10 April 1987, in the 500-km × 500-km area centered on 33°N, 23°W. The geostrophic velocity fields were calculated using centered finite differences. A mean zonal velocity component of 5 cm s^{-1} was added to these maps, as it cannot be derived from Geosat data. This describes the mean surface velocity of the Azores current observed in the region (Maillard and Käse 1989). Figure 1 shows the dynamic-topography field as derived for 10 June 1987. This field will be used in the following discussion as the reference field.

b. *Simulation of surface-drifter trajectories*

Surface-drifter trajectories were simulated from the mappings. Twenty days of drift were simulated between 31 May 1987 and 19 June 1987. Position (x_i, y_i) and float velocities (u_i, v_i) at time t_i are calculated by linear space–time interpolation. The next position is then obtained by integration (with a temporal sampling interval of 6 h). This operation is repeated to obtain the 20 days of drift. Once the drift simulation is complete, only the daily positions and velocities are retained. A minimum distance of 10 km between points is also required, since there are potential numerical difficulties in inverting the covariance matrix for the measurements if the points are too close. The velocities must therefore be considered to be mean velocities over 10-km portions of trajectories.

c. *Mapping dynamic topography by objective analysis of surface-drifter velocities*

Mapping of the dynamic surface topography H from along-trajectory velocity measurements of surface drifters ($u = u_1$, $v = u_2$), assumed to be geostrophic, was done by multivariate objective analysis. The estimation of the dynamic topography at point $\mathbf{x}$, [$\mathbf{x} = (x_1, x_2)$], $H_{\text{est}}(\mathbf{x})$ is obtained from a linear combination of observations ϕ_{obs^i}, ($i = 1, \cdots, 2N$). These are not direct measurements of H, but of the two velocity components u_{1_p} and u_{2_p} at a set of N points ($\mathbf{x}_p$) ($p = 1, \cdots, N$):

$$\phi_{\text{obs}^i} = u_1(\mathbf{x}_i) \; (i = 1, \cdots, N) \quad \text{and}$$

$$\phi_{\text{obs}^i} = u_2(\mathbf{x}_{i-N}) \; (i = N + 1, \cdots, 2N).$$

The optimal estimation and its formal error are still given by (1) and (2). Only the covariance matrices **A** and **C** are changed. They depend on covariance functions between the different variables H, u_1, and u_2. These are easy to derive from the dynamic-topography covariance function $C(r, t)$, assuming homogeneity, isotropy, and nonhorizontal divergence (geostrophy).

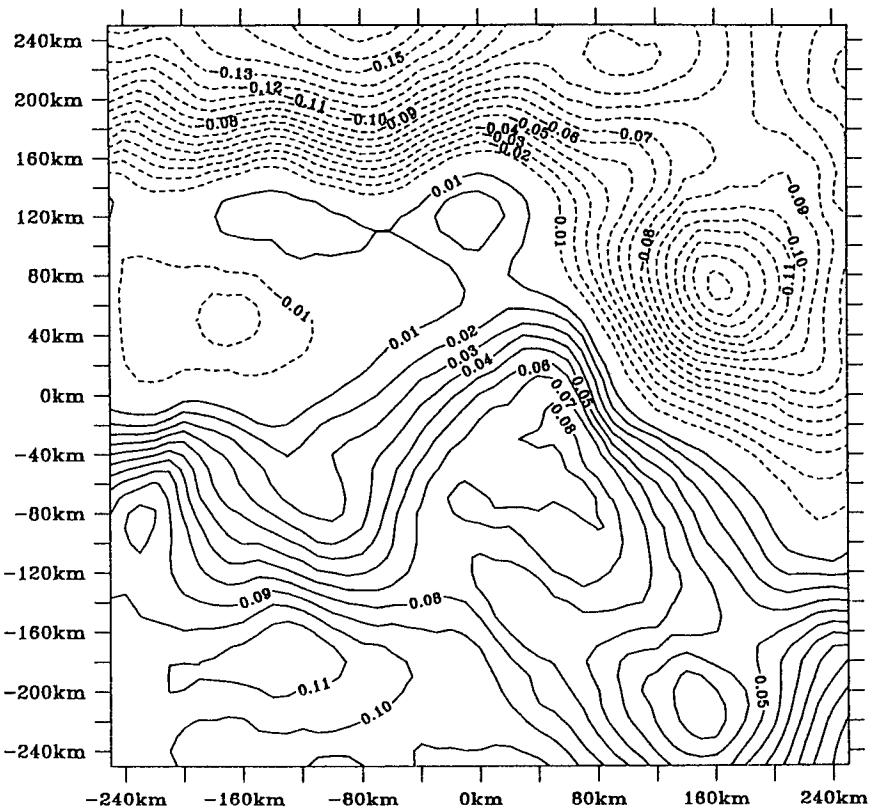

FIG. 1. Reference dynamic-topography field (m), 10 June 1987 deduced from Geosat data. The area is centered at 33°N, 23°W.

Thus, **A** and **C** can be expressed as:

$$A_{r,s} = \langle u_1(\mathbf{x}_r)u_1(\mathbf{x}_s)\rangle + \delta_{rs}E_V = \frac{(f-g)(r,t)r_1^2}{r^2} + g(r,t) + \delta_{rs}E_V$$

$$A_{r,s+N} = \langle u_1(\mathbf{x}_r)u_2(\mathbf{x}_s)\rangle = \frac{(f-g)(r,t)r_1r_2}{r^2}$$

$$A_{N+r,N+s} = \langle u_2(\mathbf{x}_r)u_2(\mathbf{x}_s)\rangle + \delta_{rs}E_V = \frac{(f-g)(r,t)r_2^2}{r^2} + g(r,t) + \delta_{rs}E_V$$

$$C_{\mathbf{x}r} = \langle H(\mathbf{x})u_1(\mathbf{x}_r)\rangle = r_2 f(r,t)k$$

$$C_{\mathbf{x}(r+N)} = \langle H(\mathbf{x})u_2(\mathbf{x}_r)\rangle = -r_1 f(r,t)k$$

$$r, s = 1, \cdots, N;$$

E_V is the velocity measurement noise variance and $k = f/g$ (g is gravity and f is the Coriolis parameter); $f(r, t) = \langle u_{//}(\mathbf{x}, t_0)u_{//}(\mathbf{x} + \mathbf{r}, t_0 + t)\rangle$ and $g(r, t) = \langle u_\perp(\mathbf{x}, t_0)u_\perp(\mathbf{x} + \mathbf{r}, t_0 + t)\rangle$ are, respectively, the velocity longitudinal and transversal covariance functions; $u_\perp$ and $u_{//}$ are the velocity components parallel and normal, respectively, to the separation vector $\mathbf{r}$ [$r = (r_1, r_2)$]; and t is the temporal lag. Parameters f and g are related to $C(r, t)$ as follows:

$$f(r,t) = -\frac{1}{r}\frac{d}{dr}\frac{C(r,t)}{k^2} \quad \text{and}$$

$$g(r,t) = -\frac{d^2}{dr^2}\frac{C(r,t)}{k^2}, \quad (4)$$

which gives

$$f(r,t) = \text{var}u\left[1 + ar - \frac{(ar)^2}{4}\right]\exp(-ar)\exp\left(\frac{-t^2}{T^2}\right) \quad (5)$$

$$g(r,t) = \text{var}u\left[1 + \frac{7(ar)^2}{4} + \frac{(ar)^3}{4}\right] \times \exp(-ar)\exp\left(\frac{-t^2}{T^2}\right); \quad (6)$$

var$u$ is the velocity variance, which does not need to be known. The analysis requires only the noise-to-signal ratio (i.e., $E_V/\text{var}u$) and the ratio var$H/\text{var}u$ which is obtained from (4) and is equal to $3k^2a^2/2$.

Note that these dynamic-topography fields will be

defined to within a constant and their mathematical expectations are, by definition, zero. These analyses are, furthermore, valid only for zero-mean fields. Before analysis, we therefore subtract the mean velocities, assumed to be known in advance or derived from the data, then analyze the velocity variations. We then add the mean dynamic topography (a north–south slope) to the result. The mean velocity is thus used simply to simulate more realistic trajectories and is used no further.

3. Results

We analyzed the dynamic topography mapped from simulated trajectories. The analyses are done for the median day, 10 June 1987. To be consistent, the objective analysis parameters are those used to calculate the initial reference field (Fig. 1), that is, $a = 40$ km^{-1} and $T = 25$ days. The percentage of noise E_V on the velocity measurements was set at 5%. This error represents the precision of daily velocity measurements by a surface drifter. Since the variance of the reference velocity-field velocity was around 65 cm^2 s^{-2} (75 cm^2 s^{-2} for the zonal component and 58 cm^2 s^{-2} for the north–south component the noise level corresponds to a realistic error on the order of 2 cm s^{-1}.

a. Mapping dynamic surface topography from nine drifters

We first released nine drifters, initially evenly spaced every 160 km. Figure 2 shows the trajectories and the mapped field. The drifter trajectories roughly follow the streamlines, since the field is nearly stationary over 20 days. There is a fairly close match to the reference field, except, of course, at places not sampled by the drifters. The discrepancy between the two fields is generally below 3 cm and has an rms value of around 1.8 cm (Fig. 3). The variance of the reference field is 16 cm^2, so the discrepancy corresponds to an error of around 20%. Although the formal mapping error decreases to 15% where the eddy is sampled by four drifters, it is, however, on average much higher (40%–50%) (Fig. 4). In fact, the nine drifters mainly sampled energetic features. In less-energetic areas, there are few measurements to constrain the analysis and a near-zero field, similar to the true field, is mapped. This explains the relatively small rms difference between the reference and estimated fields.

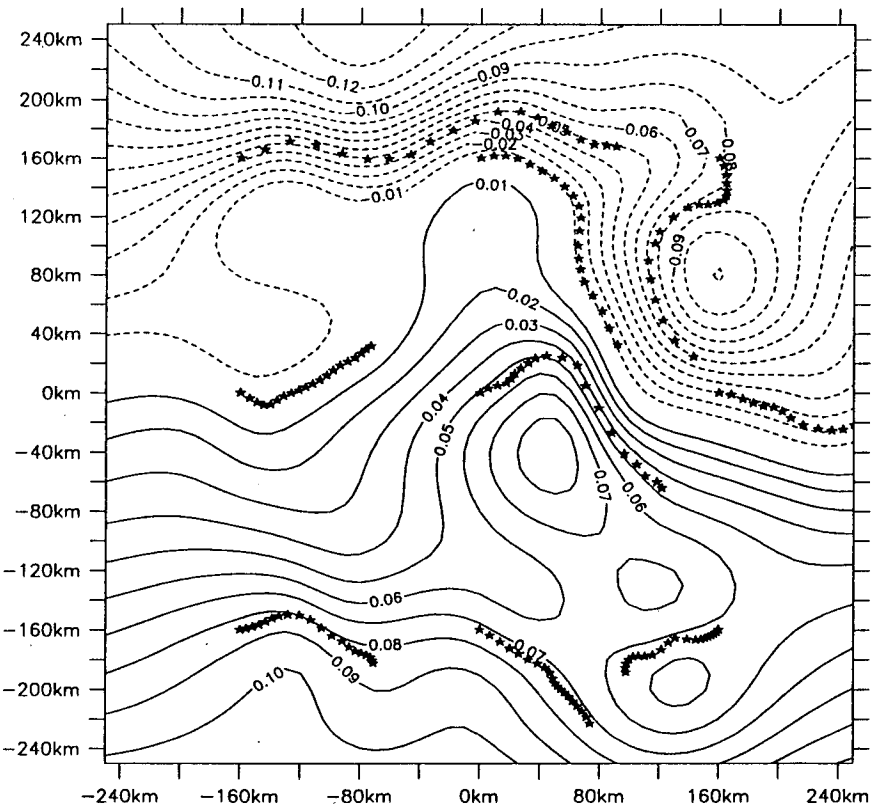

FIG. 2. Dynamic topography mapped from trajectories of nine buoys (crosses) that had drifted for 20 days around date of estimate (10 June 1987).

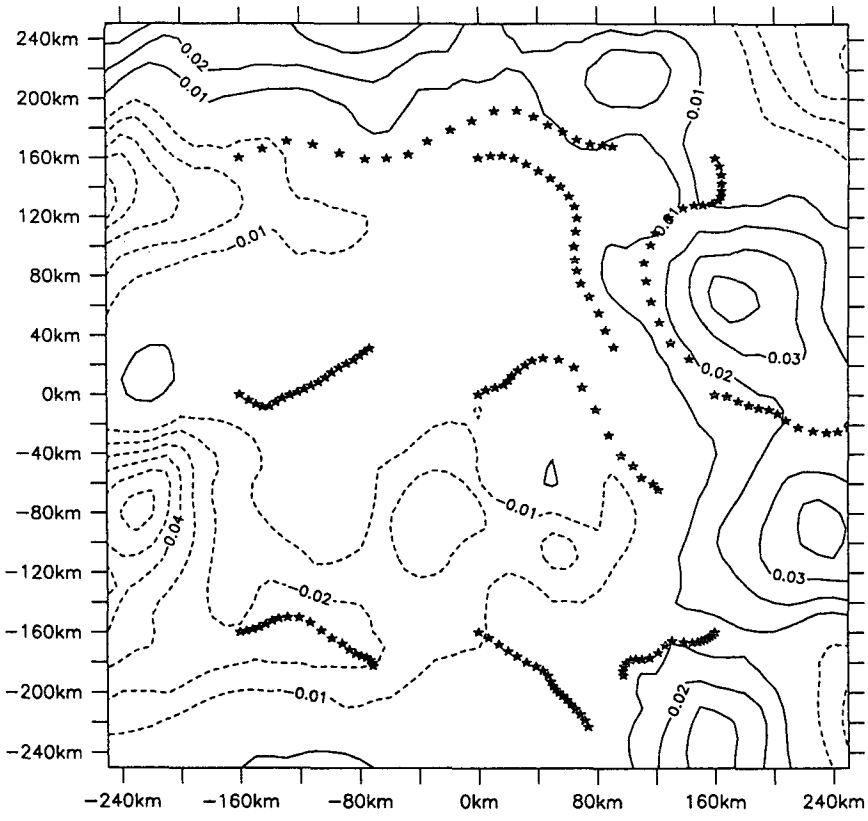

FIG. 3. Difference (m) between Fig. 2 and the reference field of Fig. 1.

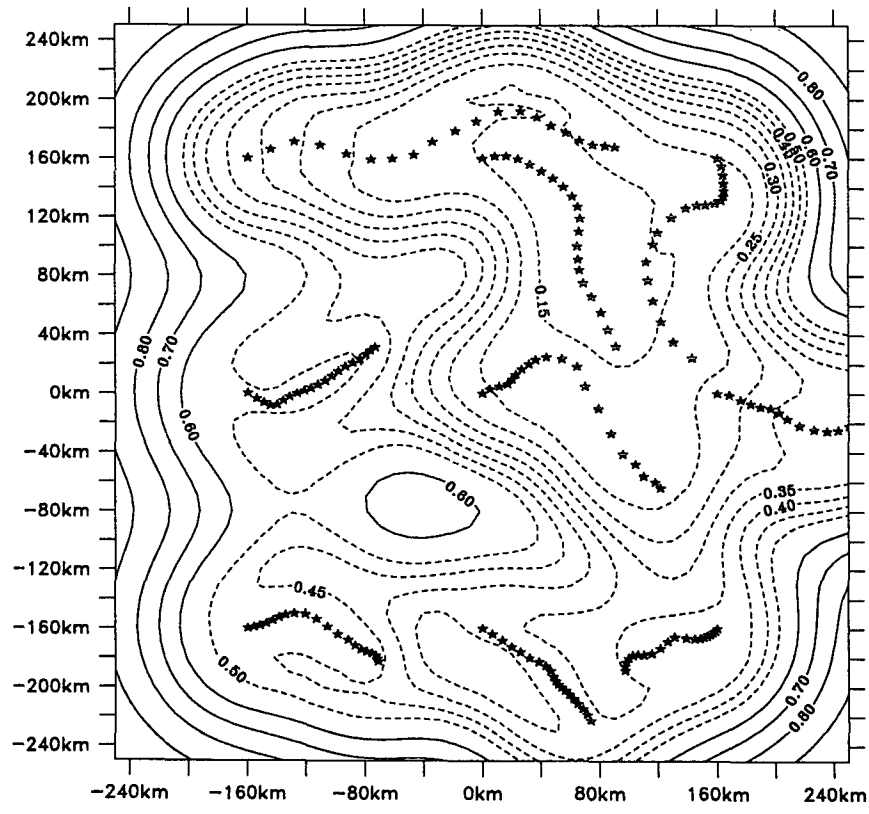

FIG. 4. Formal mapping error (percent of variance) for Fig. 2.

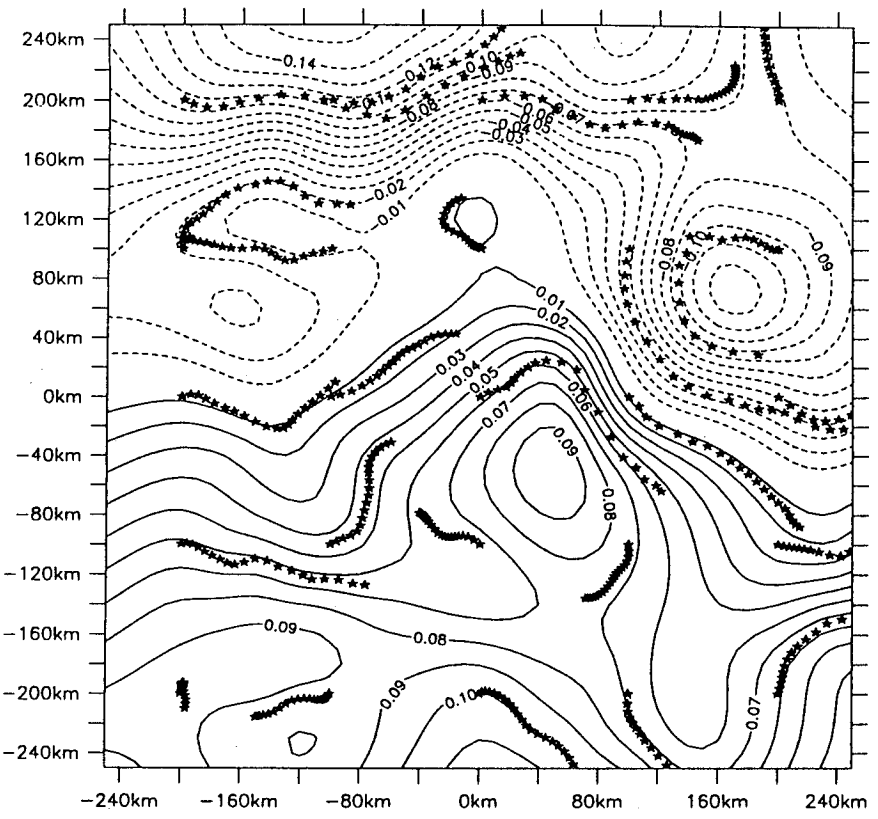

FIG. 5. Dynamic topography mapped from trajectories of 25 buoys (crosses) that had drifted for 20 days around date of estimate (10 June 1987).

b. *Mapping dynamic surface topography from 25 drifters*

Twenty-five drifters, initially evenly spaced every 100 km, produce much better mapping (Fig. 5). The rms difference with respect to the reference field is about 1.4 cm. In addition, the difference is often no more than 1 cm, apart from at the edges (Fig. 6). The formal error map (Fig. 7) gives values of 10%–20% in most of the area (which, given the signal variance, corresponds to 1.5 cm rms). Note that several drifters initially close to the edges drifted out of the box, and the velocities outside the area were not taken into account in the analysis. A similar test was done without considering a mean current. Sampling of the drifters was slightly different and there was no preferred east–west orientation of trajectories. The results were similar.

c. *Sensitivity to signal variance*

A study of sensitivity to variance level was done. We simulated new reference fields that, in relation to the reference field of Fig. 1, were four times more energetic (velocities multiplied by 2) in case (a) and a quarter as energetic (velocities divided by 2) in case (b). The dynamic topography and velocity variances are, respectively, 64 cm^2 and 260 $cm^2\ s^{-2}$ [case (a)] and 4 cm^2 and 16 $cm^2\ s^{-2}$ [case (b)]. As the reference field is obtained after objective analysis of Geosat data, its variance is probably underestimated (see, for example, Willebrand et al. 1990). The real mean situation is therefore closer to case (a), as confirmed by the variances deduced directly from along-track altimetry (Le Traon et al. 1990) or from historical surface-drifter data (Richardson 1983). The trajectories of the 25 drifters are simulated from these fields, with no mean current. To keep a constant absolute noise level with respect to the other maps mentioned, the noise level as a percentage of signal variance was set at 2.5% to 10% for cases (a) and (b), respectively. This noise level also includes variations in the number of velocity measurements on the 10-km portion of trajectory as a function of signal variance. Figures 8 and 9 are formal error maps (in percent of variance) and the simulated trajectories for cases (a) and (b). The weakest relative error is obtained for the most energetic case [case (a)] as the drifters sampled a larger area during their 20-day drift. Thus, over a large part of the area, error was lower than 10% of the signal variance. The rms difference between the mapped field and the reference field was 2.5 cm, that is, an observed error on the order of

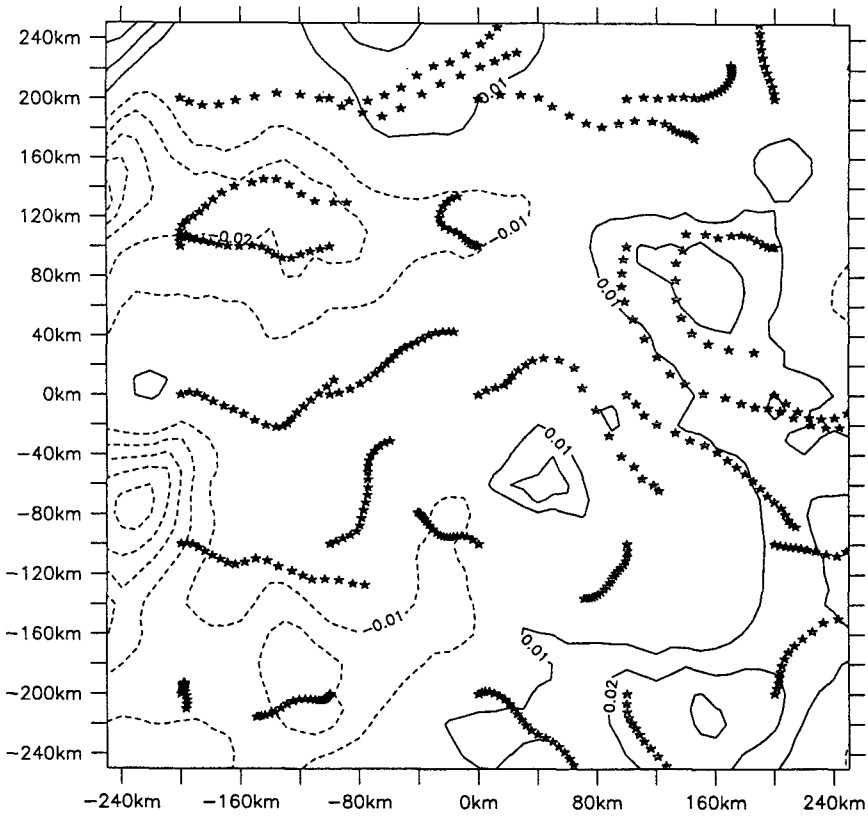

FIG. 6. Difference (m) between Fig. 5 and the reference field of Fig. 1.

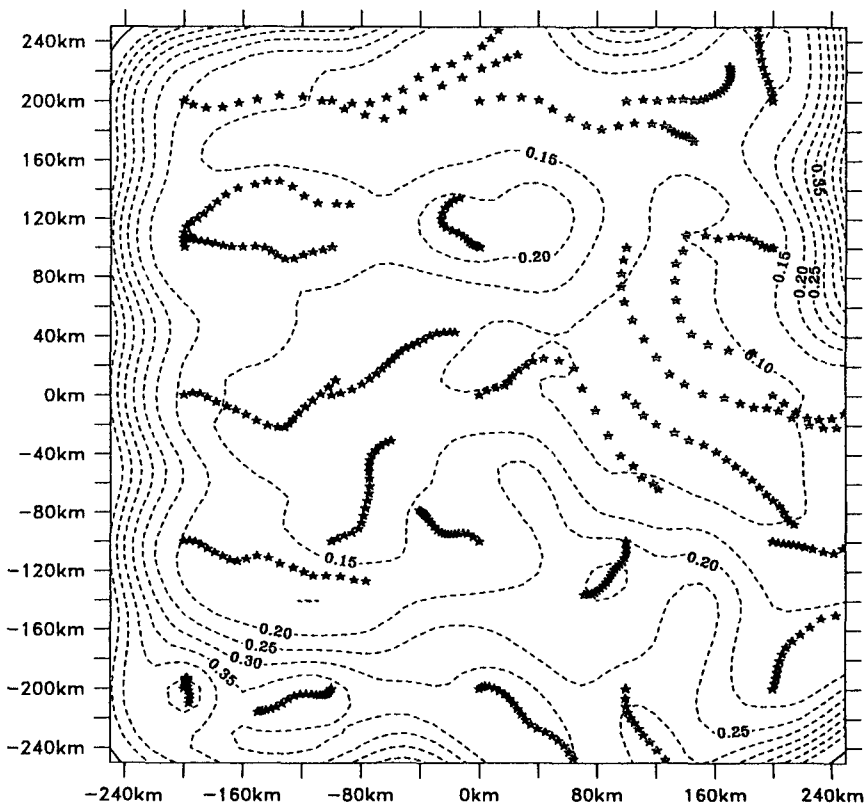

FIG. 7. Formal mapping error (percent of variance) for Fig. 5.

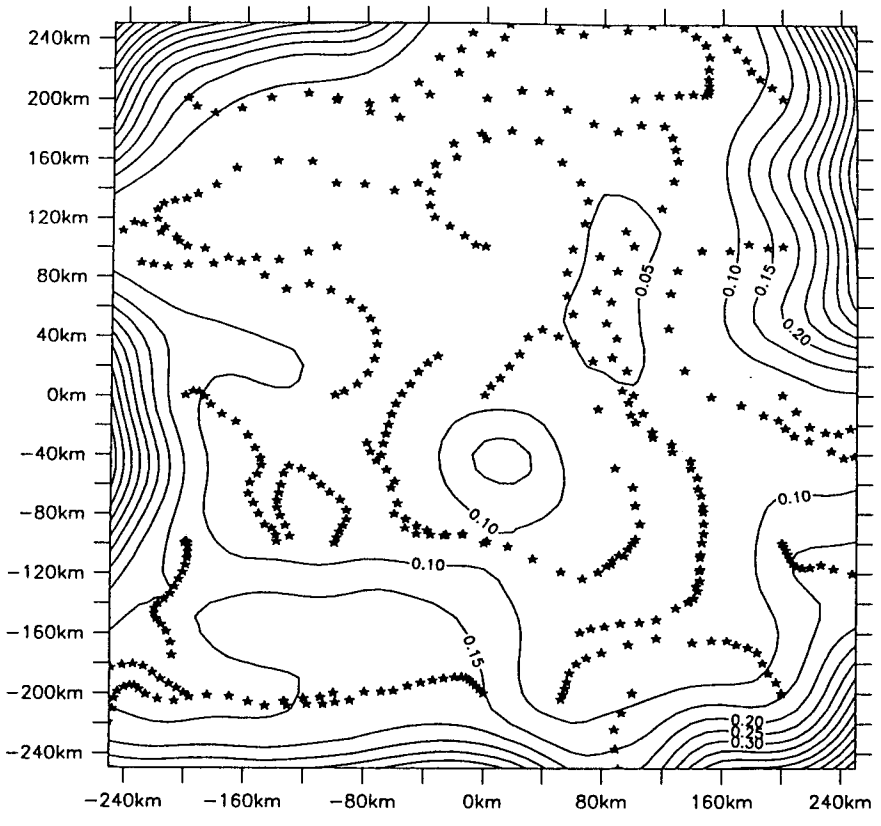

FIG. 8. Formal error on dynamic-topography mapping from 25 buoy trajectories, if energy level in reference field is multiplied by 4.

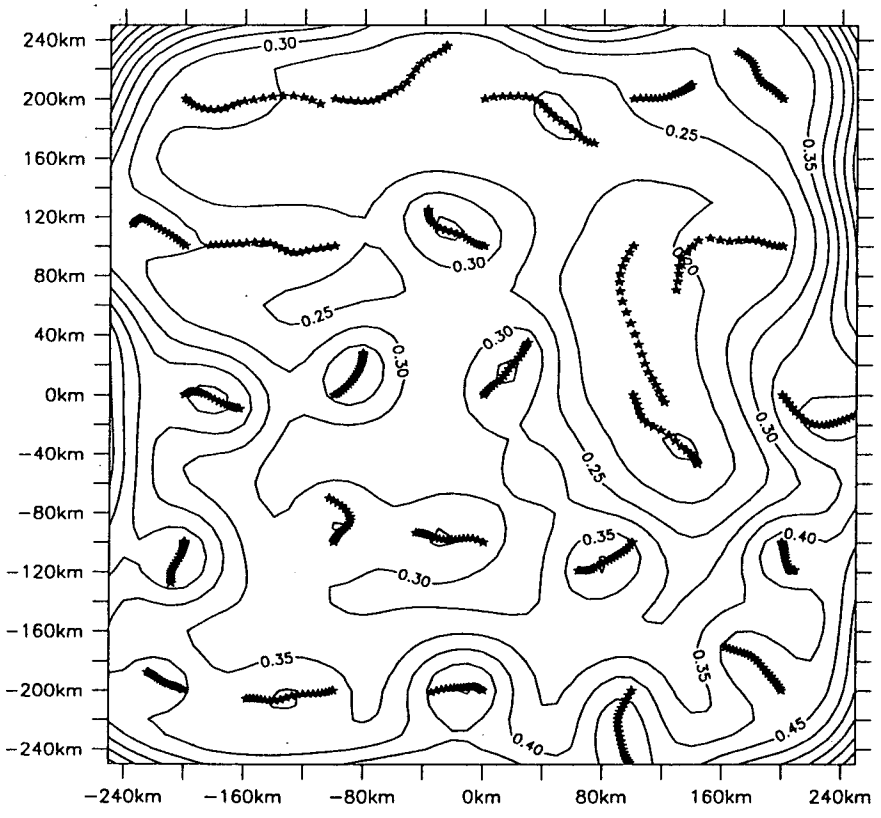

FIG. 9. Formal error on dynamic-topography mapping from 25 buoy trajectories, if energy level in reference field is divided by 4.

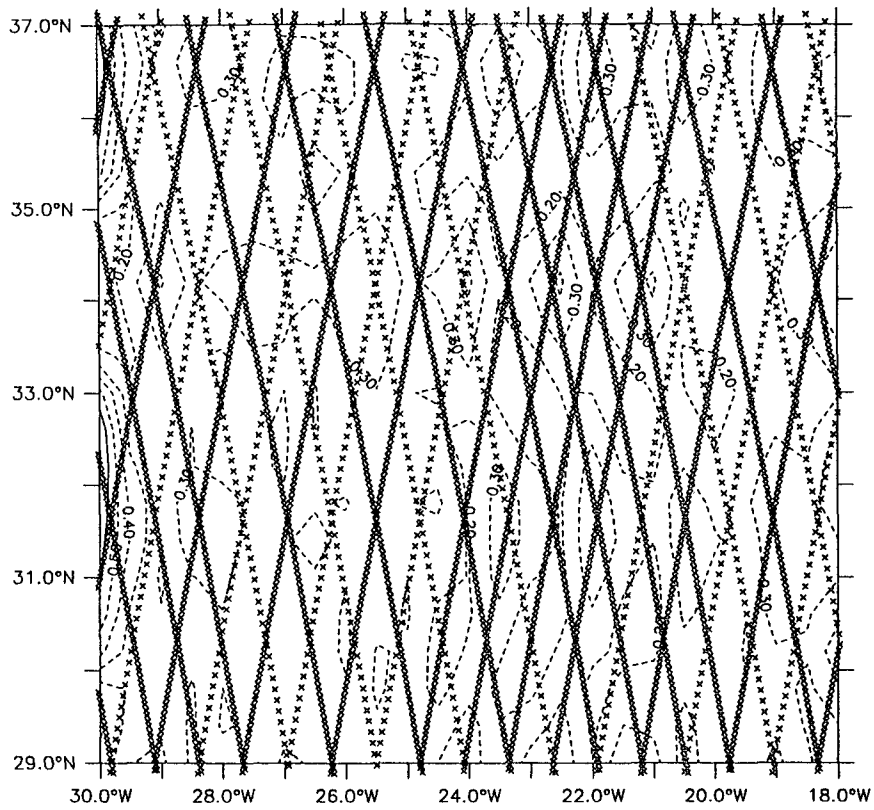

FIG. 10. Formal error (percent of variance) on dynamic topography estimated from *ERS-1* space–time coverage.

10%. The formal error is on the order of 30% for case (b), and the rms difference relative to the reference field 1 cm, that is, an observed error of 25%.

4. Comparison with satellite altimetry

The mapping of dynamic surface topography by Lagrangian drifters must now be compared with that expected from the *ERS-1* and/or TOPEX-POSEIDON satellite altimeters that are to operate during the next few years. We therefore calculated the formal error on mapping of the mesoscale variability signal using *ERS-1* data (Fig. 10), TOPEX-POSEIDON data (Fig. 11), and *ERS-1* and TOPEX-POSEIDON data combined (Fig. 12). To do this, we simulated typical *ERS-1* tracks (repeat period 35 days) and TOPEX-POSEIDON tracks (repeat period 10 days) over the area. We then estimated, by objective analysis, the formal estimation error on the dynamic topography using the method described in section 2. The estimation at a given date was done from observations spanning a ±20-day period. We sampled one point every 2 s along the track, with an associated error of 10% of the variance signal. For a 16-cm^2 signal, this corresponds to measurement noise of 1.8 cm rms for measurements averaged over a second (a somewhat optimistic view).

The formal errors for *ERS-1* are between 20% and 30%, and are relatively uniform over the area. This is due to the good space–time sampling of *ERS-1* for mesoscale features, which is in turn due to the 16-day and 19-day subcycles of the *ERS-1* orbit and to the small intertrack distance. TOPEX-POSEIDON space sampling is less suitable for two-dimensional mesoscale signal mapping (which is not the purpose of the mission). Between-track error can reach 80%. Combining *ERS-1* and TOPEX-POSEIDON data gives very good results since the error is generally between 10% and 15% of the signal variance. Thus, with 25 drifters initially spread uniformly, the results obtained are better than those with *ERS-1* or TOPEX-POSEIDON, and nearly as good as those which can be obtained by combining *ERS-1* and TOPEX-POSEIDON data (see Fig. 7). This underscores the fact that velocity measurements provide more information than dynamic topography (e.g., McWilliams 1983).

The formal errors calculated in the foregoing additionally imply that environmental corrections, orbital error, and the mean profile are known with certainty, which is, of course, not the case. Nor do they take account of the error that appears when polynomial adjustment is done to reduce the orbit error (e.g., Le Traon et al. 1991). In fact, these errors depend only

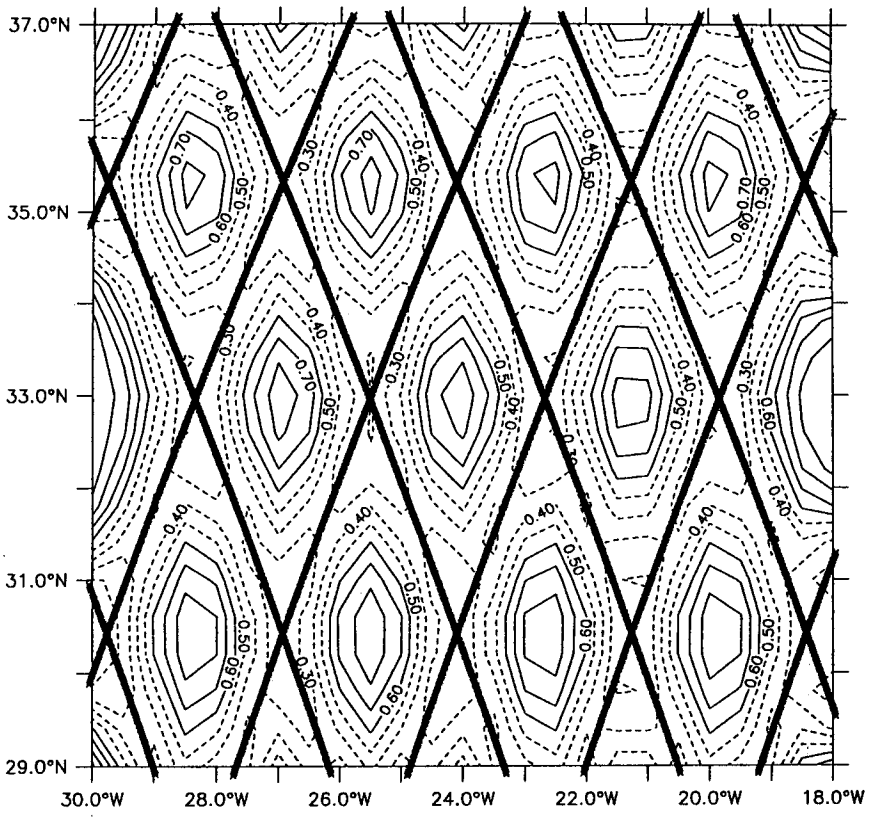

FIG. 11. Formal error (percent of variance) on dynamic topography estimated from TOPEX-POSEIDON space–time coverage.

on altimetry space–time sampling of mesoscale features. Therefore, they underestimate the true error. They are mainly useful for pointing to the threshold above which other possible sources of error may be investigated (orbit, mean profile, analysis method, environmental corrections, etc.).

The discrepancy between the dynamic topography fields derived from drifters and those derived from altimetry could also indicate residual errors in the a priori estimation of the mean circulation. The fact is that drifters measure the mean and variable circulation, while altimetry, because of the lack of precision on present geoids, gives only the variable part of the circulation. In the Azores area, however, these residual errors are probably an order of magnitude lower than the mesoscale variability signal. In addition, surface drifters need to be drogued below the Ekman layer, that is, at about 100 m or deeper, if ageostrophic effects are to be avoided. Given the vertical structure of mesoscale variability (mainly a combination of barotropic and first baroclinic mode), there should be little difference in geostrophic velocity or dynamic height between the surface and depths around 100 m. The surface mesoscale variability due to surface fronts or surface intensified eddies may, however, account for some of the difference. In any case, these small-scale structures will not be well resolved by the altimetric sampling and are likely to be smoothed out by the mapping procedure. For the validation objectives, they should be considered as additional noise in altimetric measurements.

More generally, however, the different signals and the space and time scales resolved can be estimated providing enough surface drifters are compared with the satellite altimetry. The same applies to surface drifters drogued in the mixed layer [i.e., WOCE–TOGA-type (World Ocean Climate Experiment–Tropical Ocean Global Atmosphere) drifters]. In the latter case, the comparison should allow also an estimation of ageostrophic effects.

5. Conclusions

We used Geosat data to simulate realistic drifter trajectories in the Azores area. From these trajectories, the dynamic surface topography is mapped by multivariate objective analysis to quantify the contribution of surface drifters to the description of mesoscale circulation. Lagrangian drifters strongly constrain the analysis, as they are good at sampling mesoscale features. With 25 drifters initially spread evenly through-

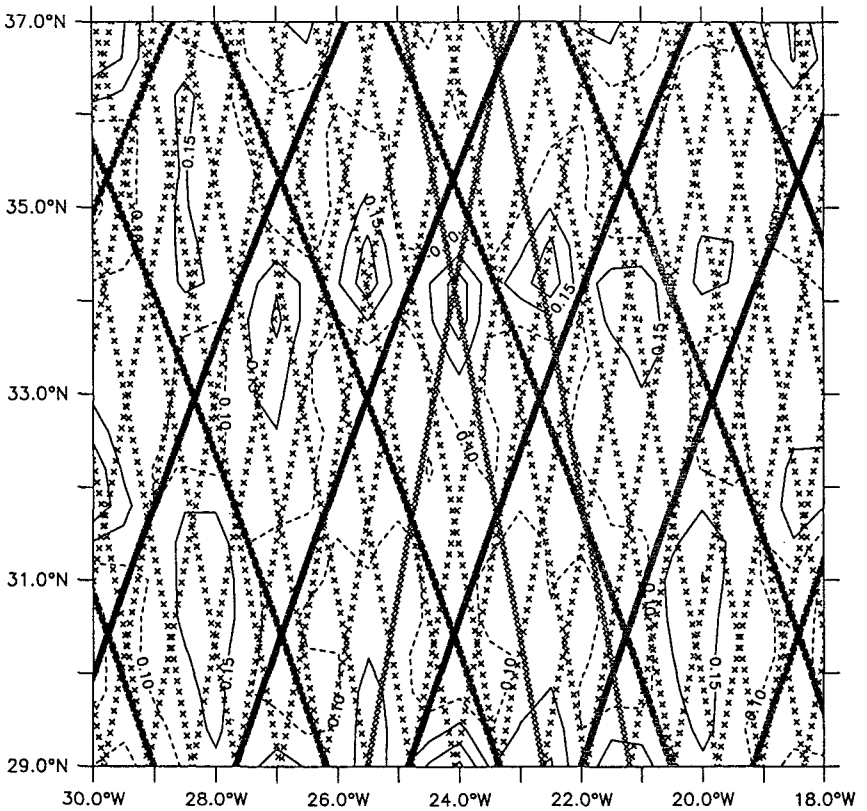

FIG. 12. Formal error (percent of variance) on dynamic topography estimated from *ERS-1* and TOPEX-POSEIDON space–time coverage.

out the area, the topography error is roughly 20% of the signal variance, and the rms discrepancy with respect to the reference altimeter field is around 1.5 cm. The error drops below 10% in areas where drifters bunch together. These results are not degraded for variances four times higher or four times lower than the variance of the reference field. The estimated error is lower than that which would be obtained from near-perfect *ERS-1* or TOPEX-POSEIDON altimetry measurements. It is of the same order of magnitude as that obtained by combining the data from the two satellites. This illustrates the usefulness of surface drifters for validating the mapping of oceanic mesoscale circulation by altimetry. More generally, it shows that by comparing satellite altimetry with data from sufficient surface drifters, the differences between the signals can be estimated. As the drifters disperse in time, the mapping will become less accurate. The sampled area will, however, become larger, enabling local comparison (and validation) over a larger area.

The study will be soon extended. First, datasets obtained after assimilation of Geosat data into models will be used. They should enhance the drifter trajectory simulations by providing a better description of small-scale (time and space) motions that are not accessible by Geosat. Tests on a larger number of configurations will then confirm these preliminary results and provide a better idea of how drifter sampling evolves over periods of a few months.

Note also that these results were obtained from an initially even spread of drifters. A better strategy would be to find the initial positions of drifters that minimize a certain cost function (e.g., the mean formal error on the 500-km × 500-km square at a given time or over a given period) given a priori knowledge of the oceanic circulation. This work is currently in progress using design experiment techniques such as those proposed by Barth and Wunsch (1990).

Acknowledgments. Geosat data were processed at GRGS/UMR39 (Groupe de Recherche en Géodésie Spatiale). We thank P. De Mey, E. Dombrowsky, P. Gaspar, and J. F. Minster for their helpful comments. This study was supported by DCN/GERDSM-CLS Contract A 91 48 619 000.

REFERENCES

Arhan, M., and A. Colin de Verdière, 1985: Dynamics of eddy motions in the eastern North Atlantic. *J. Phys. Oceanogr.*, **15**, 153–170.

Barth, N., and C. Wunsch, 1990: Oceanographic experiment design by simulated annealing. *J. Phys. Oceanogr.*, **20**, 1249–1263.

Booth, D. A., 1989: Eddies in the Rockall trough. *Oceanologica acta,* **11,** 213–218.

Bretherton, F. P., R. E. Davis, and C. B. Fandry, 1976: A technique for objective analysis design of oceanographic experiments applied to Mode 73. *Deep-Sea Res.,* **23,** 559–582.

Cheney, R. E., B. C. Douglas, R. W. Agreen, L. Miller, D. L. Porter, and N. S. Doyle, 1987: Geosat altimeter geophysical data record user handbook. National Ocean Service/NOAA, Rockville, MD.

De Mey, P., and Y. Menard, 1989: Synoptic analysis and dynamical adjustment of Geos3 and Seasat altimeter eddy fields in the north west Atlantic. *J. Geophys. Res.,* **94,** 6221–6230.

Eymard, L., 1991: The SEMAPHORE mesoscale air–sea experiment (1993). *Technical Report,* Centre de Rech. sur la Phys. de l'Environ., Issy-les-Moulineaux, France.

Gordon, A. L., and W. F. Haxby, 1990: Algulhas eddies invade the South Atlantic: Evidence from Geosat altimeter and shipboard conductivity–temperature–depth survey. *J. Geophys. Res.,* **95,** 3117–3125.

Le Traon, P. Y., 1991: Time scales of mesoscale variability and their relationship with spatial scales in the North Atlantic. *J. Mar. Res.,* **49,** 467–492.

——, M. C. Rouquet, and C. Boissier, 1990: Spatial scales of mesoscale variability in the North Atlantic as deduced from GEOSAT data. *J. Geophys. Res.,* **95,** 20 267–20 285.

——, C. Boissier, and P. Gaspar, 1991: Analysis of errors due to polynomial adjustments of altimeter profiles. *J. Atmos. Oceanic Technol.,* **8,** 385–396.

Maillard, C., and R. H. Käse, 1989: The near surface flow in the subtropical gyre south of the Azores. *J. Geophys. Res.,* **94,** 16 133–16 140.

Mc Williams, J. C., 1983: A concept of WOCE. *Large Scale Oceanographic Experiments and Satellites,* C. Gautier and M. Fieux, Eds, D. Reidel Publishing Company, 288 pp.

Niiler, P. P., R. E. Davis, and H. J. White, 1987: Water-following characteristics of a mixed layer drifter. *Deep-Sea Res.,* **34,** 1867–1882.

Richardson, P. L., 1983: Eddy kinetic energy in the North Atlantic Ocean from surface drifters. *J. Geophys. Res.,* **88,** 4355–4367.

Tapley, B. D., G. H. Born, and M. E. Park, 1982: The Seasat altimeter data and its accuracy assessment. *J. Geophys. Res.,* **87,** 3179–3188.

White, W. B., C. K. Tai, and W. R. Holland, 1990: Continuous assimilation of Geosat altimetric sea level observations into a numerical synoptic ocean model of the California current. *J. Geophys. Res.,* **95,** 3127–3148.

Willebrand, J., R. H. Käse, D. Stammer, H. H. Hinrichsen, and W. Krauss, 1990: Verification of Geosat sea surface topography in the Gulf Stream extension with surface drifting buoys and hydrographic measurements. *J. Geophys. Res.,* **95,** 3007–3014.